

## Photoelectron Angular Distributions from Above Threshold Ionization of Hydrogen Atoms in Strong Laser Fields

Lihua Bai,<sup>1,3</sup> Jingtao Zhang,<sup>1</sup> Zhizhan Xu,<sup>1,\*</sup> and Dong-Sheng Guo<sup>2,†</sup>

<sup>1</sup>State Key Laboratory of High Field Laser Physics, Shanghai Institute of Optics and Fine Mechanics, Chinese Academy of Sciences, Shanghai 201800, China

<sup>2</sup>Southern University and A&M College, Baton Rouge, Louisiana 70813, USA

<sup>3</sup>Graduate School of Chinese Academy of Science, Beijing 100049, China

(Received 22 February 2006; published 7 November 2006)

We apply a scattering theory of nonperturbative quantum electrodynamics to study the photoelectron angular distributions (PADs) of a hydrogen atom irradiated by linearly polarized laser light. The calculated PADs show main lobes and jetlike structure. Previous experimental studies reveal that in a set of above-threshold-ionization peaks when the absorbed-photon number increases by one, the jet number also increases by one. Our study confirms this experimental observation. Our calculations further predict that in some cases three more jets may appear with just one-more-photon absorption. With consideration of laser-frequency change, one less jet may also appear with one-more-photon absorption. The jetlike structure of PADs is due to the maxima of generalized phased Bessel functions, not an indication of the quantum number of photoelectron angular momentum states.

DOI: [10.1103/PhysRevLett.97.193002](https://doi.org/10.1103/PhysRevLett.97.193002)

PACS numbers: 32.80.Rm, 03.65.Nk, 12.20.Ds, 42.65.Ky

The study of photoelectron angular distributions (PADs) of above-threshold ionization (ATI) is of great importance, both theoretically and experimentally. Detailed studies on the PADs lead to significant advances in understanding the atomic dynamics in strong fields. Comparisons between theoretical results and experimental observations offer stringent tests to these various strong-field ionization theories.

Recent developments in experimental techniques made it possible to measure photoelectron kinetic-energy spectra with particularly high resolution within precisely resolved angles [1–5]. Nandor *et al.* [1] and Schyja *et al.* [5] observed a jet structure sticking out from the main lobes in the PADs of low-energy ATI peaks of xenon atoms. Here, the main lobes in PADs are the formations of photoelectrons emitted in and around the direction of laser polarization, while the jets are the formations of photoelectrons emitted from the waist between the two main lobes.

Previous experimental studies reveal that in a set of ATI peaks when the absorbed-photon number—i.e., the ATI order—increases by one, the jet number also increases by one. Since in traditional perturbation theory, a photon absorption will alter the electron angular momentum state, it is likely to attribute the number of jets in PADs to the quantum number of the electron angular momentum state. Does one more jet indicate one-more-photon absorption? Does one more jet further indicate the angular momentum quantum number change for photoelectrons? These questions will be answered in this Letter. Our theoretical study confirms this experimental observation: one more jet may appear with one-more-photon absorption; but this is not the only case. Our calculations further predict that in some cases three more jets may appear with just one-more-photon absorption. With consideration of laser-frequency

change, one less jet may also appear with one-more-photon absorption.

The nonperturbative scattering theory for multiphoton ionization (MPI) in intense laser fields of Guo, Åberg, and Crasemann (GAC) [6] is based on nonperturbative quantum electrodynamics. As a derived result, the theory finds that the (quantum-field) Volkov states are not final states, rather a set of intermediate states; while the true final electron state is an electron plane wave that follows an exit transition from the Volkov states. The early success of this theory was the interpretation of the half Kapitza-Dirac effect observed by Bucksbaum *et al.* [7,8]. Recently this theory has successfully explained the jetlike structure in PADs observed by Nandor *et al.* Our earlier study [9] showed that the PADs are determined by the generalized phased Bessel (GPB) functions and the jets feature the maxima of the GPB function [9]. A scaling law for PADs is also established [10].

In this Letter, we investigate the PADs from ATI of a H atom in strong laser fields in the frame of the nonperturbative scattering theory, which extends our previous study in PADs. Theoretically, using the H atom as a sample for calculation has a unique advantage that only one electron is in the central Coulomb field and its wave function, without interacting with light, is analytically exact. Thus, the ionization of the H atom offers an opportunity of making direct comparisons between theoretical and experimental results. We will show that, for a set of ATI peaks, with one-more-photon absorption, the number of jets in PADs does not always increase by one. Thus we see that the jetlike structure of PADs is irrelevant to the photoelectron angular momentum.

The Hamiltonian for an electron interacting with a laser field  $\mathbf{A}(\mathbf{r})$  and a spontaneously emitted mode  $\mathbf{A}'(\mathbf{r})$  is, in the units  $\hbar = c = 1$

$$H = \frac{(-i\nabla)^2}{2m_e} - \frac{e}{m_e} [(-i\nabla) \cdot \mathbf{A}(\mathbf{r}) + (-i\nabla) \cdot \mathbf{A}'(\mathbf{r})] + \frac{e^2[\mathbf{A}(\mathbf{r}) + \mathbf{A}'(\mathbf{r})]^2}{2m_e} + \omega N + \omega' N', \quad (1)$$

where  $m_e$  is the electron rest mass,  $\omega$  is the laser frequency, and photon field operators for the laser mode and the spontaneous emission, respectively, are

$$\begin{aligned} \mathbf{A}(\mathbf{r}) &\equiv g(\boldsymbol{\epsilon}\epsilon e^{i\mathbf{k}\cdot\mathbf{r}}a + \boldsymbol{\epsilon}^* e^{-i\mathbf{k}\cdot\mathbf{r}}a^\dagger), \\ \mathbf{A}'(\mathbf{r}) &\equiv g'(\boldsymbol{\epsilon}' e^{i\mathbf{k}'\cdot\mathbf{r}}a' + \boldsymbol{\epsilon}'^* e^{-i\mathbf{k}'\cdot\mathbf{r}}a'^\dagger), \end{aligned}$$

with

$$g \equiv (2V_V\omega)^{-1/2}, \quad g' \equiv (2V_V'\omega')^{-1/2},$$

and the photon number operators

$$N = \frac{1}{2}(aa^\dagger + a^\dagger a), \quad N' = \frac{1}{2}(a'a'^\dagger + a'^\dagger a').$$

In above notations, we choose the laser propagation direction  $\mathbf{k}$  as the coordinate  $z$  direction and the direction of the laser polarization  $\boldsymbol{\epsilon} = \boldsymbol{\epsilon}_x$  as the coordinate  $x$  direction. The polarization vectors of the spontaneous emission  $\boldsymbol{\epsilon}'$  has two linearly independent directions:

$$\boldsymbol{\epsilon}'_1 = \mathbf{k}' \times \boldsymbol{\epsilon}_x, \quad \boldsymbol{\epsilon}'_2 = \mathbf{k}' \times \boldsymbol{\epsilon}'_1,$$

with  $\mathbf{k}'$  being the propagation vector of the spontaneous emission. The total rate of MPI should be summed over these two directions. The wave functions of above Hamiltonian are obtained by using a quantum-field Volkov wave function, which is an eigenstate of the above Hamiltonian without  $\mathbf{A}'(\mathbf{r})$ , as the zeroth order and treating the  $\mathbf{A}'(\mathbf{r})$  terms as the perturbation. The differential ionization-rate formula, according to GAC with the inclusion of spontaneous emission, is given by [11]

$$\begin{aligned} \left. \frac{d^2W}{d^2\Omega_{\mathbf{p}_f}} \right|_j &= \frac{e^2\omega^{9/2}}{(2m_e)^{1/2}(2\pi)^5} (j - \epsilon_b - u_p)^{1/2} (j - u_p)^2 \\ &\times \sum_q (u_p - j + q) \\ &\times \int d^2\Omega_{\mathbf{k}'} |\Phi_i(\mathbf{P}_f - q\mathbf{k} + \mathbf{k}')|^2 |\mathcal{X}_q(\mathbf{P}_f, \mathbf{k}')|^2, \end{aligned} \quad (2)$$

where  $d\Omega_{\mathbf{p}_f} = \sin\theta_f d\theta_f d\phi_f$  is the differential solid angle of the final photoelectron momentum. Here  $\theta_f$  and  $\phi_f$  are the scattering angle and the azimuthal angle,  $\mathbf{P}_f$  is the final momentum of the photoelectron,  $j$  is the number of the absorbed photons for the ionization,  $\epsilon_b = E_b/\omega$  is the atomic binding energy in units of laser-photon energy, and the ponderomotive parameter  $u_p = e^2\Lambda^2/m_e\omega$  is the ponderomotive energy per laser-photon energy with  $2\Lambda$  being the classical amplitude of the laser field;  $\Phi_i(\mathbf{P}_f - q\mathbf{k} + \mathbf{k}')$  is the Fourier transform of the initial wave function. The function  $\mathcal{X}_q(\mathbf{P}_f, \mathbf{k}')$  is defined as

$$\begin{aligned} \mathcal{X}_q(\mathbf{P}_f, \mathbf{k}') &= \frac{1}{\omega} \mathcal{X}_{-j}(Z, \eta) \sum_{j'} \frac{1}{u_p - j'} \mathcal{X}_{-j'}(Z, \eta) \\ &\times \{ [ -(\mathbf{P}_f + (j - q - u_p)\mathbf{k}) \cdot \boldsymbol{\epsilon}'^* X_{q-j+j'}(Z_{k'}) \\ &+ e\Lambda \boldsymbol{\epsilon}^* \cdot \boldsymbol{\epsilon}'^* X_{q-j+j'+1}(Z_{k'}) \\ &+ e\Lambda \boldsymbol{\epsilon} \cdot \boldsymbol{\epsilon}'^* X_{q-j+j'-1}(Z_{k'}) \}, \end{aligned} \quad (3)$$

where

$$\mathcal{X}_{-j}(Z, \eta) \equiv \sum_s X_{-j+2s}(Z) X_{-s}(\eta), \quad (4)$$

is the GPB function with  $X_n(Z)$  being the phased Bessel function related to the ordinary Bessel function by

$$X_n(Z) = J_n(|Z|) e^{in \arg(Z)}.$$

The arguments of the GPB function are

$$\begin{aligned} Z_f &= 2 \frac{|e|\Lambda}{m_e\omega} \mathbf{P}_f \cdot \boldsymbol{\epsilon}, & Z_{k'} &= 2 \frac{|e|\Lambda}{m_e\omega} \mathbf{k}' \cdot \boldsymbol{\epsilon}, \\ Z &= Z_f + Z_{k'}, & \eta &= \frac{1}{2} u_p \cos\xi, \end{aligned} \quad (5)$$

where the angle  $\xi$  monitors the polarization degree such that  $\xi = 0$  denotes the linear polarization and  $\xi = \pi/2$  the circular polarization. The PAD represents the relative ionization rate for different azimuths at a fixed scattering angle.

In our calculations, the PADs are obtained from Eq. (2) at the fixed scattering angle  $\theta_f = \pi/2$  and a varying azimuthal angle  $\phi_f$  from  $0^\circ$  to  $180^\circ$  with a step size  $6^\circ$ . The initial momentum-space wave function of an H atom in its ground state is given by

$$\Phi_i(\mathbf{P}_i) = \frac{2^3(\pi a_0^3)^{1/2}}{(1 + P_i^2 a_0^2)^2},$$

where  $a_0$  is the Bohr radius, with the corresponding binding energy 13.6 eV. The laser light is linearly polarized and of different wavelengths. We find that the PADs of H atoms show the main lobes and jet structures.

We first calculate the PADs of a H atom irradiated by the laser light of wavelength 700 nm. We find that at certain laser intensities the number of jets increases one with absorbing one more photon, as shown in Fig. 1, for a set of ATI peaks at laser intensity  $1.5 \times 10^{13}$  W/cm<sup>2</sup>. For 700 nm laser light each laser photon has energy 1.8 eV. With overcoming the ponderomotive shift in addition to the binding energy, the ground-state electron has to absorb nine photons to form the first ATI peak, ten photons to form the second ATI peak, and so on. Figure 1 describes the polar plots of the calculated PADs for the second, the third, and the fourth ATI peaks, respectively. Each plot shows the main lobes in the laser-polarization direction and several jets sticking out from the waist between the main lobes. There are five jets sticking out from the second ATI peak, six from the third one, and seven from the fourth one; even though the jets may be too small to see clearly in the

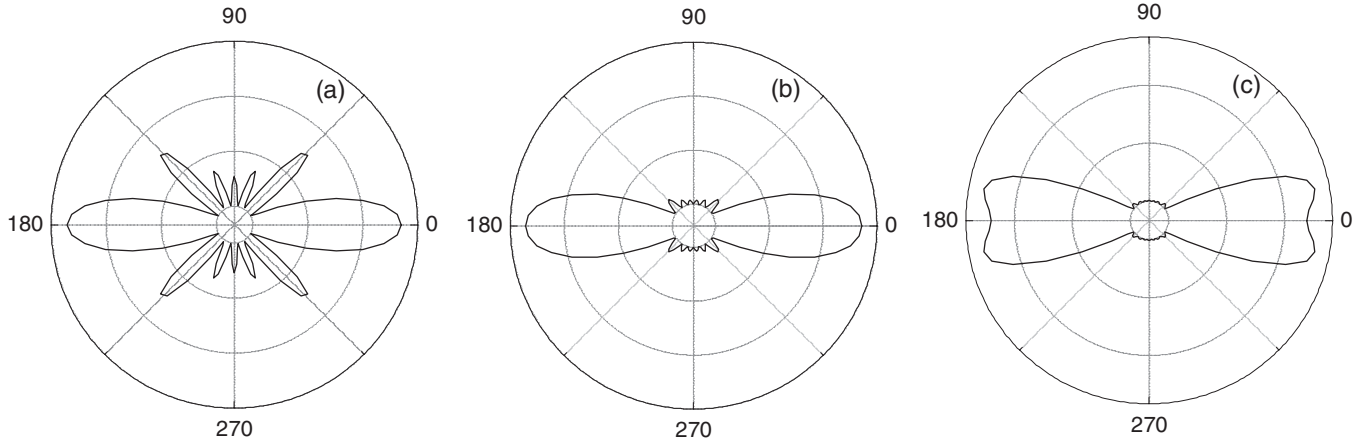


FIG. 1. Polar plots of the calculated PADs of (a) the second; (b) the third, and (c) the fourth ATI peaks. The laser intensity is  $1.5 \times 10^{13}$  W/cm<sup>2</sup>, and the laser wavelength is 700 nm.

plots. Here the number of jets refers to that in one side of the PADs. In a general sense, Fig. 1 shows that when one more photon is absorbed, the number of jets of corresponding PADs increases by one. This feature does agree with the observation of Nandor *et al.* [1]. Moreover, a central jet appears in the PADs of the second and the fourth ATI peaks, since they are of the even-number photon process.

According to the analysis made by Zhang *et al.* [9], the jets in PADs feature the maxima of the GPB function, and the total number of jets on one side of the PADs is twice the number of maxima in the domain of the first variable. Here the GPB function means the one as the leading factor in Eq. (3) in front of the summation symbol. The value of GPB function increases oscillatorily with the increasing angular variable at a fixed laser intensity; thus, has many extrema. The laser intensity affects the PADs via the ponderomotive parameter  $u_p = e^2 \Lambda^2 / m_e \omega = 2\pi e^2 I / m_e \omega^3$ . The oscillation pattern of the GPB function on  $Z$  variable

varies with the value of  $u_p$ , which is determined by the laser intensity and laser frequency. We can obtain various PADs by changing the laser intensity and/or the laser frequency.

So far, the calculations show that the number of jets increases by one with absorption of one more photon in a set of ATI peaks. In the following, by comparing an  $n$ -photon PAD with its neighboring  $(n + 1)$ -photon PAD, we show that the number of jets may increase by one, and by three (but not two), and may decrease by one with also the laser-frequency change. In Fig. 2, we depict the PADs for the first four ATI peaks at laser intensity  $1 \times 10^{12}$  W/cm<sup>2</sup> and wavelength 780 nm. For the first ATI peak, the PAD aligns with the laser-polarization direction. For the small value of the photoelectron momentum, the first argument of the corresponding GPB function could not reach any maximum of the GPB; then, there is no jet in the PAD, as shown in Fig. 2(a). For the other three ATI peaks, there are, respectively, three, six, and seven jets in

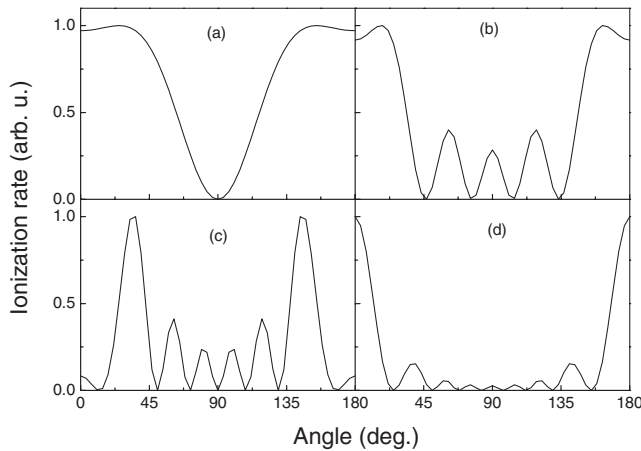


FIG. 2. PADs for (a) the first, (b) the second, (c) the third, and (d) the fourth ATI peaks. The laser field intensity is  $1 \times 10^{12}$  W/cm<sup>2</sup> and the laser wavelength is 780 nm. Each PAD is normalized by its maximum, respectively.

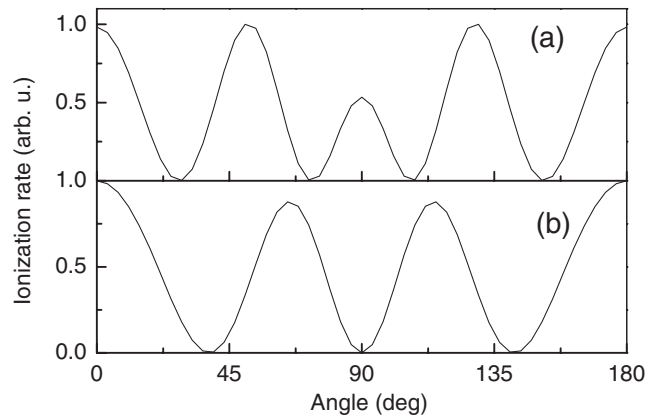


FIG. 3. PADs for the first ATI peak in laser fields of equal intensity ( $6 \times 10^{11}$  W/cm<sup>2</sup>) but different wavelength: (a) 650 nm and (b) 780 nm. Each PAD is normalized by its maximum, respectively.

TABLE I. All possible numbers of jets for each ATI peak. The two calculated jet-number changes (5, 6, 7) and (0, 3, 6, 7) are denoted by underlines, which correspond to the jet-number changes in Fig. 1 and 2, respectively. From the Table, we may see other possible jet-number changes.

ATI order	Absorbed photon number $j$	Possible number of jets 0 1 2 3 4 5 6 7 8 9 10 11 ...
1	9	<u>0</u> 2 4 6 8 10 . . . . .
2	10	1 <u>3</u> <u>5</u> 7 9 11 . . . . .
3	11	0 2 4 <u>6</u> 8 10 . . . . .
4	12	1 3 5 <u>7</u> 9 11 . . . . .

the PADs according to ATI order, even though the number of the absorbed photons increases by moving to the next ATI peak. Among the first four ATI peaks, only the second one and the fourth one have the central jet. This is due to the even number of absorbed photons.

Our calculations also show that the number of jets may decrease when one more photon is absorbed. A sample calculation is presented in Fig. 3, where the PADs of the first ATI peak in two different laser frequencies are depicted. The laser intensity is chosen as  $6 \times 10^{11}$  W/cm<sup>2</sup>, and the laser wavelengths are 650 and 780 nm, respectively. Figure 3(a) describes the PAD of an eight-photon ATI peak, showing three jets. Figure 3(b) describes a PAD of a nine-photon ATI peak, but showing two jets. This comparison provides an example of when the number of absorbed photons increases the number of jets may decrease. Even though these two ATI peaks do not belong to the same set of ATI peaks, this example still shows that the number of jets is not directly related to the absorbed-photon number. This prediction can be tested by future experiments. Moreover, a central jet appears in the PAD of the eight-photon ATI and no central jet in the PAD of the nine-photon ATI, which is consistent with our earlier analysis [9].

From the above calculation results, we see that one more jet may not indicate one-more-photon absorption. Does one more jet further indicate the angular momentum quantum number change for photoelectrons according to the traditional perturbation theory? The three-more-jet case shows that the number of jets does not indicate the angular momentum change. From our calculation, the value of  $|Z_f|_{\max} = \sqrt{8u_p(j - u_p - \epsilon_b)}$  determines the number of jets. According to our number rule, the total number of jets on one side of the PADs is twice the number of maxima in the domain  $(0, |Z_f|_{\max})$ . The quantity  $8u_p(j - u_p - \epsilon_b)$  varies with laser frequency and intensity. On Table I we list all possible numbers of jets, in principle, for each ATI peak. We denote the two calculated jet-number changes (5, 6, 7) and (0, 3, 6, 7). From Table I, we may see other possible jet-number changes that can be studied in the future.

In summary, the number of jets in PADs from ATI of a hydrogen atom in strong linearly polarized laser fields varies with the laser intensity and the laser frequency through the quantity  $8u_p(j - u_p - \epsilon_b)$ . When the number of absorbed photons increases by one, the number of jets does not always increase by one. It may increase by three or other odd numbers, even decrease by one. This study illustrates that the jetlike structure of PADs is irrelevant to the photoelectron angular momentum.

This work is supported by the national Basic Research Program of China, the Chinese National Natural Science Foundation, and the Major Basic Research Project of Shanghai. Zhang is sponsored by the Shanghai Rising-Star Program.

\*Electronic address: zzxu@mail.shcnc.ac.cn

†Electronic address: dsquo@grant.phys.subr.edu

- [1] M. J. Nandor, M. A. Walker, and L. D. Van Woerkom, *J. Phys. B* **31**, 4617 (1998).
- [2] B. Yang, K. J. Schafer, B. Walker, K. C. Kulander, P. Agostini, and L. F. Dimauro, *Phys. Rev. Lett.* **71**, 3770 (1993).
- [3] M. Lewenstein, K. C. Kulander, K. J. Schafer, and P. H. Bucksbaum, *Phys. Rev. A* **51**, 1495 (1995).
- [4] S. Dionissopoulou, T. Mercouris, A. Lyras, and C. A. Nicolaides, *Phys. Rev. A* **55**, 4397 (1997).
- [5] V. Schyja, T. Lang, and H. Helm, *Phys. Rev. A* **57**, 3692 (1998).
- [6] Dong-Sheng Guo, T. Åberg, and B. Crasemann, *Phys. Rev. A* **40**, 4997 (1989).
- [7] P. H. Bucksbaum, D. W. Schumacher, and M. Bashkansky, *Phys. Rev. Lett.* **61**, 1182 (1988).
- [8] Dong-Sheng Guo and G. W. F. Drake, *Phys. Rev. A* **45**, 6622 (1992).
- [9] Jingtao Zhang, Wenqi Zhang, Zhizhan Xu, Xiaofeng Li, Panming Fu, Dong-Sheng Guo, and R. R. Freeman, *J. Phys. B* **35**, 4809 (2002).
- [10] Dong-Sheng Guo, Jingtao Zhang, Zhizhan Xu, Xiaofeng Li, Panming Fu, and R. R. Freeman, *Phys. Rev. A* **68**, 043404 (2003).
- [11] J. Gao, Dong-Sheng Guo, and Yong-Shi Wu, *Phys. Rev. A* **61**, 043406 (2000).